

Adsorption and mechanism study for methyl orange dye by cross-linked chitosan-ethylene glycol diglycidyl ether beads

Ali H. Jawad*

Faculty of Applied Sciences, Universiti Teknologi MARA, 40450 Shah Alam, Selangor, Malaysia, emails: ahjm72@gmail.com/
ali288@salam.uitm.edu.my

Received 10 November 2018; Accepted 7 June 2019

ABSTRACT

In this study, cross-linked chitosan-ethylene glycol diglycidyl ether beads (Chi-EGDEB) were prepared to be potential adsorbent for methyl orange (MO) dye removal from aqueous solution. Adsorption experiments were performed as a function of contact time (0–240 min), initial dye concentration (50–200 mg/L), and pH (3–10). The adsorption data of MO on the cross-linked Chi-EGDEB were in agreement with Langmuir and Freundlich isotherms. The adsorption capacity of the cross-linked Chi-EGDEB for MO was 112.4 mg/g at 303 K. The kinetic data were well described by pseudo-second-order kinetic model. The adsorption process was spontaneous and endothermic in nature. The mechanism of adsorption included mainly hydrogen bonding interaction, electrostatic attractions, and $n-\pi$ stacking interaction. This study reveals that the cross-linked Chi-EGDEB as a good candidate for removal of acid dye from aqueous solution.

Keywords: Chitosan beads; Ethylene glycol diglycidyl ether; Cross-linking; Adsorption; Methyl Orange

1. Introduction

Due to the fast industrialization, the addition of various types of pollutants to the water system is one of the common problems worldwide. Dyes are recalcitrant and stable toward the environment and some of them are also carcinogenic and teratogenic offering significant risk to the aquatic species and human beings [1,2]. Adsorption is a convenient and well-known technique that is commonly applied in the removal of dyes compared with other dye removal methods such as advanced oxidation process, electrochemical destruction, Fenton reaction, oxidation, ozonation, photochemical, ultraviolet irradiation, and adsorption have been established in countless research papers claiming successful dye removal [3]. Biopolymers are better described as the naturally occurring polymers produced by living species with molecular backbones composed of repeating units of saccharides, nucleic acids, and sometimes various

additional chemical side chains contributing to variance in their functionalities [4,5].

Chitosan (Chi) is a well-known cationic polysaccharide and abundantly available low-cost biopolymer. Chi is an ideal adsorbent for removal of unlimited numbers of water pollutants and various classes of textile and food dyes [5]. The presence of free amino ($-\text{NH}_2$) and hydroxyl ($-\text{OH}$) groups in the molecular structure of Chi can effectively serve as active adsorption sites. The protonation of amino groups in acidic media is responsible for increasing the electrostatic attraction toward anionic dyes [6]. However, due to the solubility of raw Chi in many organic acids and high swelling capacity in water, compressible at high operating pressure, low mechanical strength, and low surface area limit the application of this material in water treatment technologies [7].

Several modification methods have been made in order to improve the physicochemical properties of Chi, which generally involved physical modification [8], chemical

* Corresponding author.

modification [9], and photo transformation [10]. Chemical cross-linking reaction is one of the convenient and practical ways to improve physical/mechanical properties of Chi, and reduce its degree of swelling and leachability in aqueous system [11]. The cross-linking step is responsible for reducing the adsorption capacity of Chi, if amine groups are involved in cross-linking reaction. However, this limiting effect of chemical cross-linking significantly depends on the physiochemical properties and concentration of cross-linking agent, and procedure used for cross-linking reaction [12].

Dialdehyde cross-linking agents are commonly applied in cross-linking of Chi. However, the adsorption capacity would be greatly decreased by cross-linking reaction, because the cross-linking agent mainly reacts with $-NH_2$ groups, and as a result, the residual $-NH_2$ functional groups are reduced [9]. The concentration of cross-linking agent is a key factor to dominate the adsorption capacity of the cross-linked Chi. Therefore, at low concentrations of cross-linking agent, a higher adsorption capacity will be obtained due to more availability of free $-NH_2$ functional groups present in the Chi backbone [11]. Diepoxy cross-linking agents such as ethylene glycol diglycidyl ether (EGDE) can play a significant role to interlink Chi at its backbone by joining more Chi macromolecules together to increase the molecular weight, and to enhance the physicochemical property of Chi [13].

Adsorption is a surface phenomenon and can be occurred by the donor/acceptor complexation mechanism where atoms of the surface functional group donate electrons to the sorbate molecules [14]. Even though, the adsorption capacity of cross-linked Chi expected to be lower than unmodified Chi due to blocking of some functional groups by cross-linking reaction, mainly amine ($-NH_2$) groups. On the other hand, the adsorption capacity on cross-linked Chi can be also enhanced by increasing the molecular size after binding with cross-linking agent. In addition to improve the functionality, hydrogen bonding ability, and Chi chain branching by cross-linking reaction. Therefore, the objective of this work is to produce cross-linked chitosan-ethylene glycol diglycidyl ether (CS-EGDEB) as a low-cost and environment friendly synthetic biopolymer for removal of acid dye from aqueous solution. The cross-linking reaction was carried out at low cross-linking concentration and at mild condition. Methyl Orange (MO) with poly aromatic rings and complicated molecular structures was selected as model pollutants to examine the adsorptive behavior of Chi-EGDEB.

2. Materials and methods

2.1. Materials

Chitosan (Chi) (68.2% degree of deacetylation), and ethylene glycol diglycidyl ether (EGDE) solution were purchased from Sigma-Aldrich, Malaysia. Methyl Orange (MO) was purchased from ACROS, Organics, and chemical formula: $C_{14}H_{14}N_3NaO_3S$, MW: 327.32, $\lambda_{max} = 465$ nm). Hydrochloric acid (HCl), sodium hydroxide (NaOH), and other reagents utilized in this work were all of analytical grade. The stock solution with ultra-pure water was used throughout the experiments.

2.2. Preparation of Chi-EGDEB

2 g of Chi flakes was dissolved in 70 mL of 5% acetic acid solution. The viscous solution of Chi was left under gentle stirring for 24 h until all the Chi flakes were completely dissolved. The beads were formed by dropping the Chi gel solution into 0.05 M NaOH solution by using 10 mL syringe (TERUMO, Malaysia, 10 cc/mL). The hydrogel beads were washed using distilled water until natural pH was reached. After that, 200 mL of 1% (v/v) of EGDE solution was added to the Chi beads and stirred for 4 h at $40^\circ\text{C} \pm 2^\circ\text{C}$. Then, the cross-linked Chi-EGDE beads were washed, dried, and sieved to a constant size of 250–500 μm before use.

2.3. Characterization of Chi-EGDEB

The surface morphology of the cross-linked Chi-EGDEB was examined *via* scanning electron microscope (SEM, Zeiss Supra 40 VP, Germany). Elemental analysis was carried out by CHNS-O analyzer (Flash 2000, Organic Elemental Analyzer, Thermo-Scientific, Netherland). The functional groups of the cross-linked Chi-EGDEB before and after MO adsorption were identified by Fourier transform infrared (FTIR) Spectroscopy (PerkinElmer, Spectrum RX I, USA). X-ray diffraction (XRD) was performed in order to determine the crystallinity or amorphous nature by XRD in reflection mode (Cu $K\alpha$ radiation) on an X'Pert Pro X-ray diffractometer (PANalytical). Textural characterization of cross-linked Chi-EGDEB was carried out by N_2 adsorption using Micromeritics ASAP 2060, USA.

2.4. Batch equilibrium study

The adsorption of MO on the cross-linked Chi-EGDEB was investigated in batch experiments mode. The experiments were carried out in a series of 250-mL Erlenmeyer flask containing 100 mL of MO solution with different initial MO concentrations (50–200 mg/L). The dosage of cross-linked Chi-EGDEB ranging from 0.05 to 0.5 g in 100 mL were added to the MO solution with pH varied from 3 to 10 and agitated with fixed shaking speed of 90 strokes/min at 303 K by using a thermostat shaker (Memmert waterbath model WNB7-45, Germany). After shaking the samples, the adsorbent was separated by centrifuged (KUBOTA model 2800 at 2,400 rpm for 10 min. The solution pH was adjusted with 0.10 M NaOH or HCl by using a pH meter (Metrohm, 827 pH lab). The change in MO concentration was determined using a HACH DR 2800 (USA) direct reading spectrophotometer at a maximum wave length of 465 nm. The effect of temperature on MO uptake was performed by following the same procedures at 303, 313, and 323 K. The adsorption capacity at equilibrium, q_e (mg/g), and the percentage of dye removal (DR %) of studied dyes were determined using Eqs. (1) and (2), respectively.

$$q_e = \frac{(C_0 - C_e)V}{W} \quad (1)$$

$$\text{DR}\% = \frac{(C_0 - C_e)}{C_0} \times 100 \quad (2)$$

C_0 : initial concentrations of the MO (mg/L); C_e : liquid-phase concentrations of the MO (mg/L) at equilibrium; V : volume of the MO solution (L); W : dried weight of the cross-linked Chi-EGDEB (g).

3. Results and discussion

3.1. Characterization of the cross-linked Chi-EGDEB

3.1.1. XRD analysis

The XRD pattern of the cross-linked Chi-EGDEB is shown in Fig. 1. XRD pattern is indexed based on a standard diffraction reference pattern (JCPDS no. 89-8487). Appearance of a broad diffraction background and the absence of a sharp peak reveal a partially crystalline structure polysaccharide due to its regular chain and have a single reflection fall at $2\theta = 24^\circ$ in the spectrum. The signature at 2θ assigned to the crystal form was enhanced in the cross-linked Chi-EGDEB after cross-linking reaction with EGDE.

3.1.2. Elemental and surface area analysis

The elemental analysis (CHN) result of the cross-linked Chi-EGDEB is given in Table 1. It was found that content carbon, hydrogen, and nitrogen content is quite comparable with the unmodified Chi [7], and the changes in the elements content were minor at the best. This observation indicates that the cross-linking reaction with EGDE at low concentration did not alter much the molecular structure of Chi. As for textural properties, cross-linked Chi-EGDEB has a low BET surface area of $0.39 \text{ m}^2/\text{g}$. Pore sizes are classified in accordance with the IUPAC classification system (USA), where pores may possess variable diameter (d): micropores ($d < 2.0 \text{ nm}$), mesopores ($2.0 \text{ nm} < d < 50 \text{ nm}$), and macropores ($d > 50 \text{ nm}$). The textural properties are listed in Table 1 and clearly indicate that cross-linked Chi-EGDEB is a mesoporous material.

3.1.3. FTIR spectral analysis

FTIR spectral analysis of the cross-linked Chi-EGDEB before adsorption (Fig. 2a), and after MO adsorption (Fig. 2b)

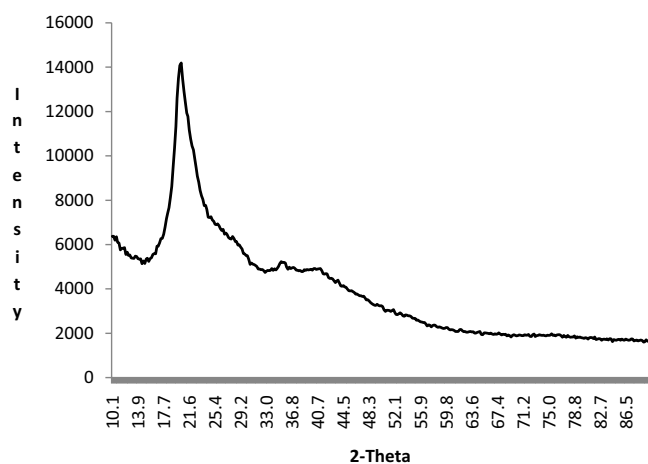


Fig. 1. XRD pattern of cross-linked Chi-EGDEB.

Table 1

Elemental analysis results for cross-linked Chi-EGDEB

Elemental analysis (wt.%)	Value
C%	38.30
H%	7.40
N%	5.23
O% (by difference)	49.07
Textural properties	
Total pore volume ($p/p^0 = 0.990$) (cm^3/g)	0.0011
BET surface area (m^2/g)	0.39
Mean pore diameter (nm)	11.28

was performed. From Fig. 2a, the characteristic bands of the cross-linked Chi-EGDEB shown at $\sim 3,400 \text{ cm}^{-1}$ (O–H and N–H stretching vibration), $\sim 2,800 \text{ cm}^{-1}$ (C–H stretching vibrations in –CH and –CH₂) [14]. A band at $\sim 1,650 \text{ cm}^{-1}$ (Vibration of N–H band). Other bands at $\sim 1,420 \text{ cm}^{-1}$ (–NH₂ bending vibration of the primary amino group), and $\sim 1,050 \text{ cm}^{-1}$ (C–O–C stretching vibration of pyranose ring) [15,16]. After MO adsorption (Fig. 2b), a new band appears at $\sim 1,500 \text{ cm}^{-1}$ (C=C stretch in aromatic ring) can be assigned to the poly aromatic ring of MO dye loaded onto the cross-linked Chi-EGDEB.

3.1.4. SEM analysis

SEM analysis was carried out to examine the surface morphology of the cross-linked Chi-EGDEB before and after adsorption. Fig. 3a shows top-view image of the cross-linked Chi-EGDEB particle at magnification power $150\times$. As can be seen, the cross-linked Chi-EGDEB particle is semi-spherical in shape. The external surface of the cross-linked EGDEB was further examined at higher magnification power $1,000\times$ as shown in Fig. 3b. According

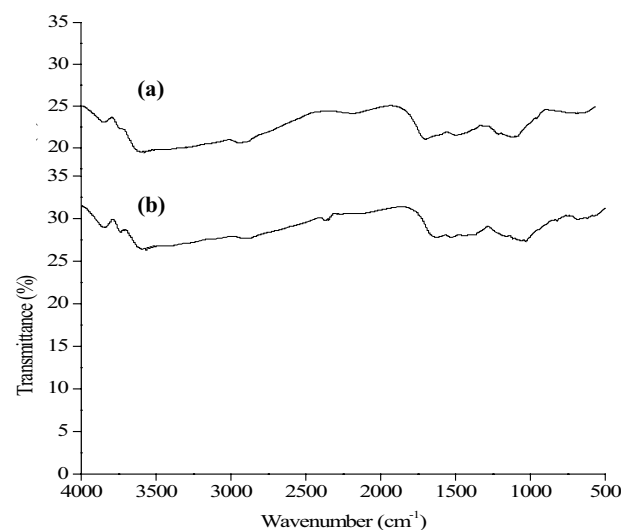


Fig. 2. FTIR spectral analysis for (a) cross-linked Chi-EGDEB and (b) cross-linked Chi-EGDEB after MO adsorption.

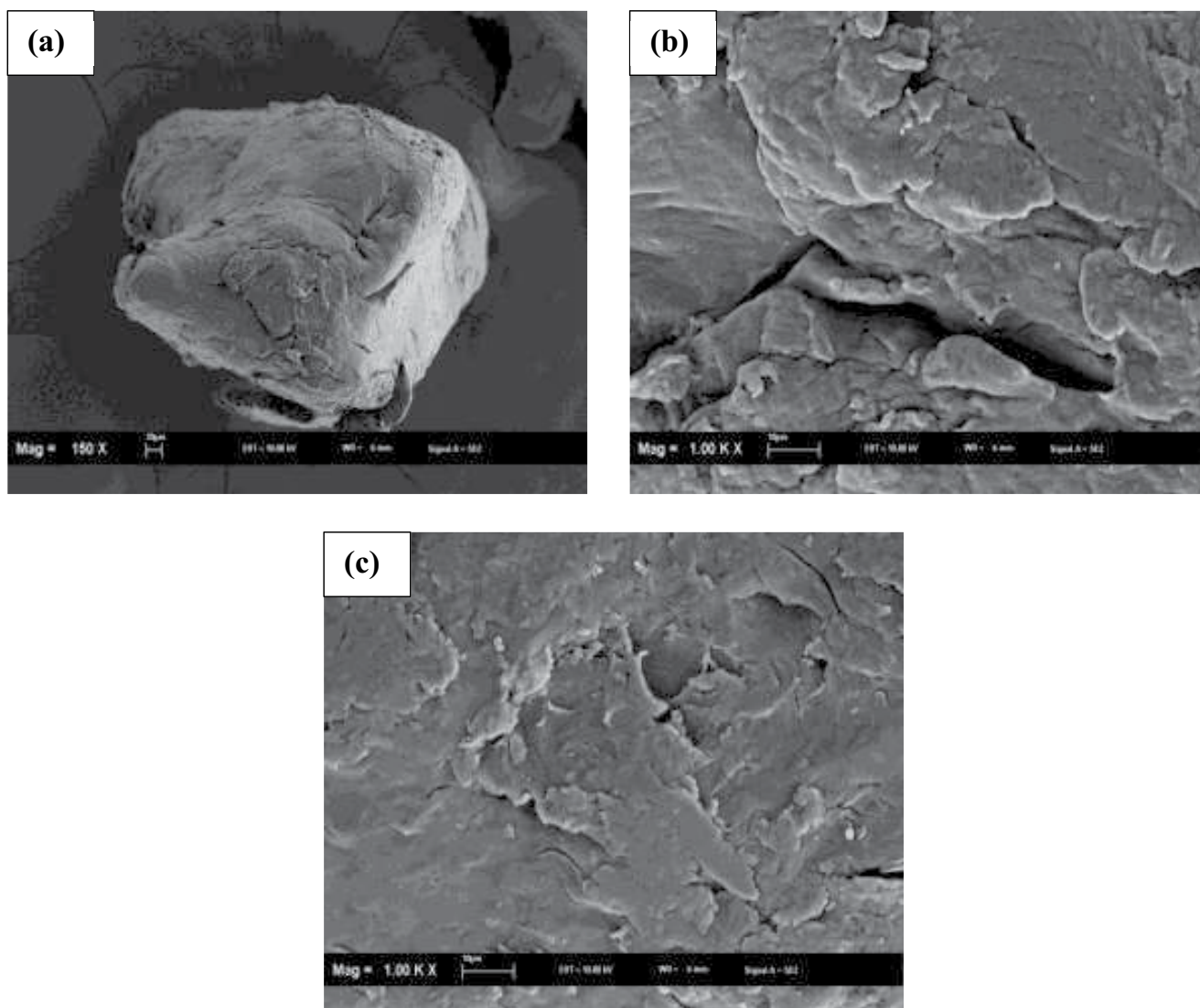


Fig. 3. SEM images for (a) the top-view of the cross-linked Chi-EGDEB particle at 150 \times , (b) surface of the cross-linked Chi-EGDEB particle at 1,000 \times , and (c) surface of the cross-linked Chi-EGDEB particle at 1,000 \times after MO adsorption.

to Fig. 3b, the surface features of the cross-linked are well-pronounced heterogeneous cavities that distributed across the cross-linked Chi-EGDEB surface. Therefore, the SEM image reveals that MO may be adsorbed onto the cross-linked Chi-EGDEB surface and the accessible pore domains of the carbonaceous surface. The surface morphology of the cross-linked Chi-EGDEB after MO adsorption is shown in Fig. 3c. As can be seen, Fig. 3c reveals a change in the topography of the adsorbent, as evidenced by the appearance of reduced cavities size and compact surface features due to the loading of MO dye molecules on the surface of the cross-linked Chi-EGDEB.

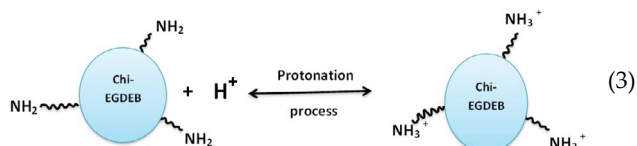
3.2. Batch adsorption study

3.2.1. Effect of solution pH

The acidity of the medium is one of the most significant parameters in adsorption. Therefore, the effect of initial

solution pH on the MO uptake by the cross-linked Chi-EGDEB was evaluated within pH range between 3 and 11 is shown in Fig. 4. It was evident that the maximum MO uptake was observed at pH 3, and gradual decreases in the MO uptake can be observed by increasing the pH value toward basic environment.

In fact, in acidic environment the surface of the cross-linked Chi-EGDEB will be positively charged due to the protonation of amine groups ($-\text{NH}_2$) on the surface of the cross-linked Chi-EGDEB [6,8,17]. This protonation process is responsible for producing more cationic amines groups on the surface of the protonated cross-linked Chi-EGDEB (Eq. (3)):



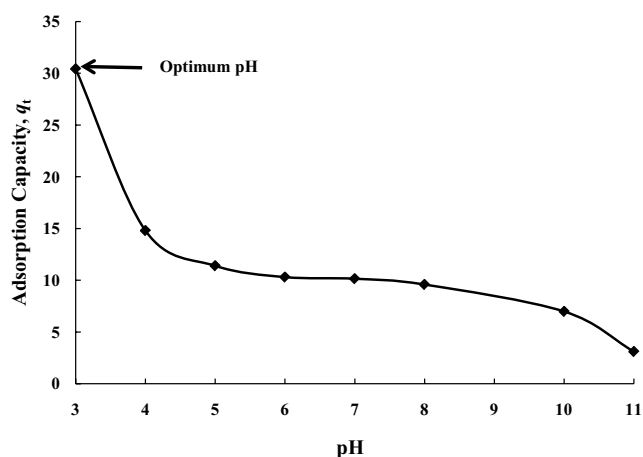
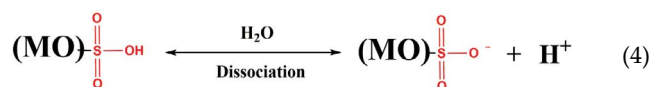
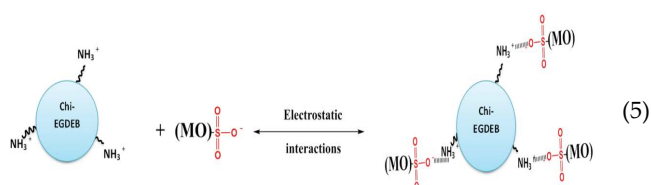


Fig. 4. Effect of solution pH on the MO uptake onto cross-linked Chi-EGDEB at $[MO] = 100$ mg/L, temperature 303 K, and mass of adsorbent 0.3 g/100 mL.

On the other hand, the sulfonate group ($-SO_3H$) in the molecular structure of the MO dye can be converted in aqueous medium into active negative sulfonate group ($-SO_3^-$) (Eq. (4)).



Consequently, a strong electrostatic (coulombic) attraction between positively charged protonated amino group of the cross-linked Chi-EGDEB with negatively charged sulfonate group of MO, thus increases dye adsorption (Eq. (5)).



Moreover, the decreasing in the adsorption capacity of the cross-linked Chi-EGDEB with increasing pH value can be attributed to the competition between anionic dyes and excess OH^- ions in the solution. Therefore, the initial pH ~ 3 of the MO solution was selected for further studies.

3.2.2. Effect of the cross-linked Chi-EGDEB dosage

The quantity of the available sorbent in the liquid phase is an important parameter that strongly affects dye uptake. Various dosage amounts of the cross-linked Chi-EGDEB ranging from 0.05 to 0.5 were added to the 100 mL of 100 mg/L of MO solution. The effect of the cross-linked Chi-EGDEB dosage on MO removal is shown by Fig. 5. It is apparent that by increasing the cross-linked Chi-EGDEB dosage from 0.05 to 0.3 g, the percentage of MB removal increased from 16.6% to 47.1%. It was also observed from Fig. 5 that the increase in the MO removal as the cross-linked

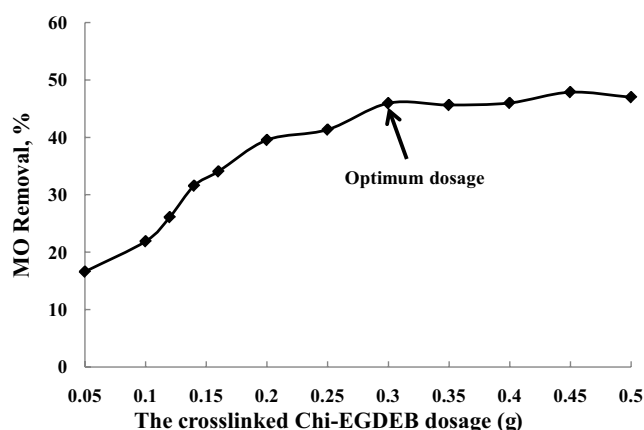


Fig. 5. Effect of adsorbent dosage on the MO removal and amount of adsorbed MO on the cross-linked Chi-EGDEB ($[MO] = 100$ mg/L and temperature 303 K).

Chi-EGDEB was increased due to the increase in the surface area of available cross-linked Chi-EGDEB in solution. A higher adsorbent dosage also reflects a greater number of active adsorption sites available. Therefore, 0.30 g/100 mL was selected for further adsorption studies.

3.2.3. Effect of C_0 and contact time

The influence of contact time and initial MO concentration (50–200 mg/L) on the adsorption capacity of the cross-linked Chi-EGDB is shown in Fig. 6. The experimental data reveal that the adsorption capacity at equilibrium increases from 16.6 to 60.6 mg/g, with increase in the initial MO concentration from 50 to 200 mg/L. This was attributed to a greater collision rate between dyes molecules and the cross-linked Chi-EGDEB by increasing the initial MO concentration. Furthermore, the time to reach equilibrium also increased with the increase in initial MO concentration. It follows that the MO shows the tendency to move deeper from the surface of the cross-linked Chi-EGDEB to access the active adsorption sites.

3.3. Kinetic modeling

In order to figure out the adsorption mechanism, the non-linear pseudo-first-order (PFO) model and pseudo-second-order (PSO) models were used to test the experimental data of initial concentration. The Lagergren [18] PFO model is expressed by Eq. (6):

$$q_t = q_e (1 - \exp^{-k_1 t}) \quad (6)$$

The non-linear form of the PSO model [19] is described by Eq. (7):

$$q_t = \frac{q_e^2 k_2 t}{1 + q_e k_2 t} \quad (7)$$

q_e : amounts of dyes adsorbed by the cross-linked Chi-EGDEB at equilibrium; q_t : amounts of dyes adsorbed by the

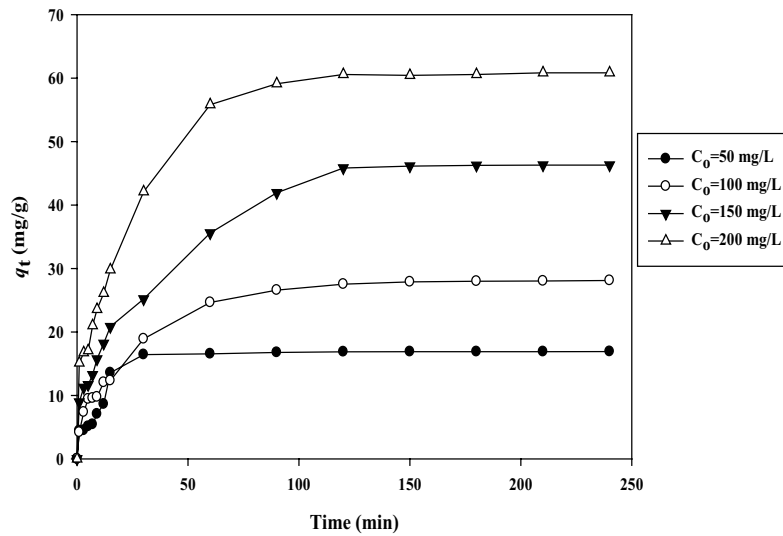


Fig. 6. Effect of initial dye concentrations and contact time on the uptake of MO onto cross-linked Chi-EGDEB (pH = 3, temperature = 303 K, and mass of adsorbent 0.3 g/100 mL).

cross-linked Chi-EGDEB at time t ; k_1 : PFO rate constant (1/min); k_2 : PSO rate constant (g/mg min); t : time (min).

The kinetic data were fit using the non-linear form of the PFO and PSO models, where the best fit was estimated by coefficient of determination (R^2) represented by Eq. (8) [20] as follows:

$$R^2 = 1 - \frac{\sum_{n=1}^n (q_{t,meas} - q_{t,cal})^2}{\sum_{N=1}^N (q_{t,cal} - q_{t,cal})^2} \quad (8)$$

$q_{t,meas}$ and $q_{t,cal}$ are the measured and calculated adsorption capacity at time t , and n is the number of observations. Fig. 7 shows the predicted PFO and PSO models for MO adsorption on the cross-linked Chi-EGDEB by the use of

non-linear method. Additionally, the kinetic parameters of these two models at variable concentration along with the corresponding values of R^2 are listed in Table 2. The kinetic parameters are recorded in Table 2. From Table 2, it was found that the adsorption of MO dye by the cross-linked Chi-EGDEB follows the PSO model in terms of higher correlation coefficient values R^2 . An accurate fit to the PSO kinetic model suggests that chemisorption is the possible rate-determining step that controls the adsorption process, where the adsorption rate of MO is proportional to the number of active sites available on the cross-linked Chi-EGDEB [21].

3.4. Isotherm modeling

The adsorption isotherm is the most meaningful information which describes how the adsorbate molecules

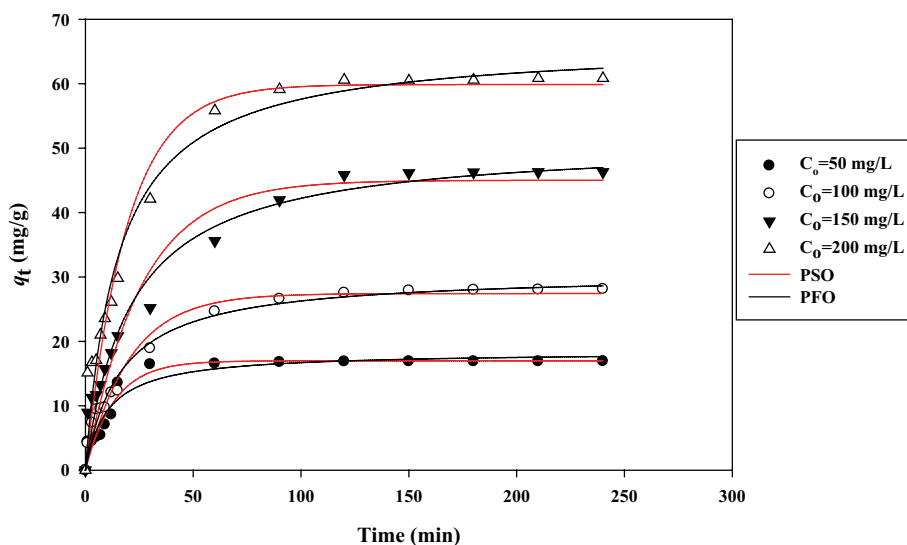


Fig. 7. Non-linear plots of PFO and PSO models for MO adsorption on the cross-linked Chi-EGDEB.

Table 2

PFO and PSO kinetic parameters values for adsorption of MO on the cross-linked Chi-EGDEB

[MO] ₀ (mg/L)	<i>q_{e,exp.}</i> (mg/g)	PFO		
		<i>q_{e,cal.}</i> (mg/g)	<i>k₁</i> (min ⁻¹) × 10 ⁻²	<i>R</i> ²
50	16.8	16.9	7.49	0.95
100	28.6	27.4	4.88	0.96
150	46	45	3.89	0.95
200	60.6	59.8	5.20	0.96
[MO] ₀ (mg/L)	<i>q_{e,exp.}</i> (mg/g)	PSO		
		<i>q_{e,cal.}</i> (mg/g)	<i>k₁</i> (min ⁻¹) × 10 ⁻³	<i>R</i> ²
50	16.8	18.4	5.34	0.97
100	28.6	30.5	2.0	0.98
150	46	51.1	0.99	0.97
200	60.6	62.4	0.92	0.97

distribute between the solid–liquid phases when the adsorption process reaches an equilibrium state. Various isotherm models such as Langmuir, Freundlich, and Temkin were used to explain the equilibrium characteristics of adsorption. The Langmuir isotherm model [22] describes the monolayer adsorption process on uniform adsorption sites and is expressed by Eq. (9) as follows:

$$q_e = \frac{q_{\max} K_a C_e}{1 + K_a C_e} \quad (9)$$

q_e: Adsorbed amount of dyes at equilibrium (mg/g); *C_e*: dye concentration at equilibrium (mg/L); *q_{max}*: Langmuir maximum adsorption capacity (mg/g); *K_a*: Langmuir constant (L/mg).

The equilibrium data were also fitted to the Freundlich isotherm model [23], which is expressed by Eq. (10) as follows:

$$q_e = K_f C_e^{1/n} \quad (10)$$

K_f: adsorption capacity (mg/g); *1/n*: adsorption intensity of the system.

Temkin isotherm [24] model takes into account the heat of adsorption of all molecules in the layer which would decrease linearly rather than logarithmic with coverage [25]. The model is given by Eq. (11) as follows:

$$q_e = \frac{RT}{b_T} \ln(K_T C_e) \quad (11)$$

K_T: Temkin isotherm constant (L/mg); *R*: universal gas constant [8.314 J/(mol K)]; *T*: (K) is the absolute temperature (K); *b_T*: heat of adsorption (J/mol).

The non-linear plots of the tested isotherms models relate to Eqs. (9)–(11) are presented in Fig. 8, where the corresponding isotherm parameters are recorded in Table 3. According to high *R*² values (Table 3), the Langmuir and Freundlich models provide a satisfactory fit to the isotherm results. It can be inferred that adsorption takes place at homogeneous and heterogeneous surface sites

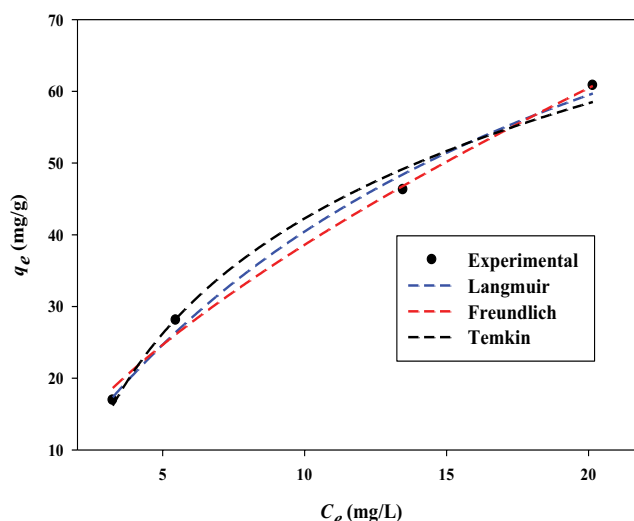


Fig. 8. Langmuir, Freundlich, and Temkin isotherm plots for the adsorption of MO on the cross-linked Chi-EGDEB at 303 K.

Table 3

Isotherm parameters of the Langmuir, Freundlich, and Temkin models for MO adsorption on cross-linked Chi-EGDEB at 303 K.

Adsorption isotherms	Value
Langmuir	
<i>q_m</i> (mg/g)	112.4
<i>K_a</i> (L/mg)	0.056
<i>R</i> ²	0.99
Freundlich	
<i>K_f</i> (mg/g)	8.69
<i>n</i>	1.54
<i>R</i> ²	0.99
Temkin	
<i>K_T</i> (L/mg)	11.2
<i>b_T</i> (J/mol)	106.8
<i>R</i> ²	0.92

that are energetically equivalent. The cross-linked Chi-EGDEB shows good adsorptive property toward MO dye with relatively high adsorption capacity of 112.4 mg/g. The adsorption capacity of MO by cross-linked Chi-EGDEB was compared with various adsorbents as given in Table 4. From Table 4, it can be concluded that the cross-linked Chi-EGDEB possesses a relatively high adsorption capacity, suggesting that it may be a promising material for the removal of acid dyes from aqueous solutions.

3.5. Adsorption mechanism

The proposed adsorption mechanism of MO on the cross-linked Chi-EGDEB is illustrated in Fig. 9. According to the available functional groups on the surface of Chi-EGDEB, the adsorption mechanism of MO on the cross-linked Chi-EGDEB can be assigned to the various interactions, for example, hydrogen bonding interaction (Fig. 9a), electrostatic attractions (Fig. 9b), and $n-\pi$ stacking interaction (Fig. 9c). Furthermore, the electrostatic interaction between negatively charged sulfonate (SO_3^-) acid group of MO and the positively charged cross-linked Chi-EGDEB improved the adsorption. In this respect, Heibati et al. [37] attributed the possible adsorption mechanism of Reactive Black 5 by pumice and walnut activated carbon to the electrostatic attractions between positively charged adsorbents and negatively charged adsorbate. Another important factor for MO adsorption by the cross-linked Chi-EGDEB is the $n-\pi$ stacking interaction (Fig. 9c). In fact, the $n-\pi$ interaction generally occurred where the lone pair electrons on an oxygen atom are delocalized into the π orbital of an aromatic ring of dyes [38].

3.6. Adsorption thermodynamics

Adsorption thermodynamics of MO on the cross-linked Chi-EGDEB was determined from the experimental data obtained at various temperatures of 303, 313 and 323 K and the thermodynamic parameters, such as Gibb's free energy

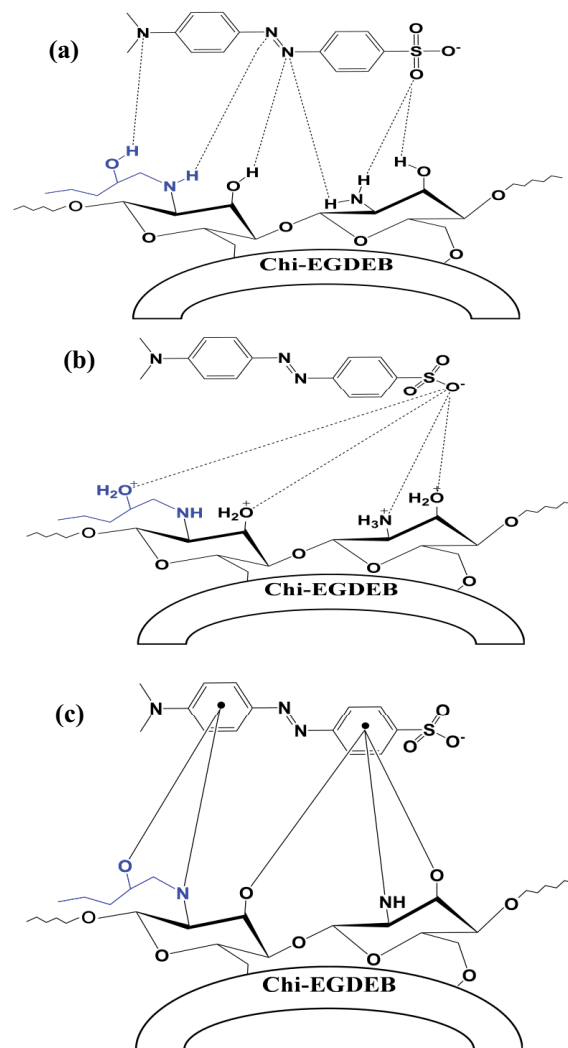


Fig. 9. Schematic illustration of various types of interactions between MO and the cross-linked Chi-EGDEB: (a) hydrogen bonding, (b) electrostatic bonding, and (c) $n-\pi$ interactions.

Table 4
Adsorption capacities for MO by various adsorbents

Adsorbent	q_{\max} (mg/g)	pH	Reference
Chi-EGDEB	112.4	4	This study
Magnetic chitosan beads	779	4	[26]
Cross-linked chitosan/ TiO_2 nanocomposite	416.1	4	[27]
Lapindo volcanic mud	333.3	3	[28]
Chitosan microspheres	207	3.1	[29]
Chitosan-EGDE biofilm	131.2	4	[30]
Protonated cross-linked chitosan	95.69	4.5	[31]
$m\text{-CS}/\gamma\text{-Fe}_2\text{O}_3/\text{MWCNTs}$	66.09	3.14–6.5	[32]
Chitosan/Kaolin/ $\gamma\text{-Fe}_2\text{O}_3$ nanocomposites	37	7	[33]
Chitosan	34.83	4	[34]
Chitosan/alumina composite	33	6	[35]
Maghemite/chitosan films	29	3	[36]

Table 5

Thermodynamic parameters for the adsorption of MO on cross-linked Chi-EGDEB

T (K)	$\ln k_d$	$\Delta G_{\text{ads}}^{\circ}$ (kJ mol ⁻¹)	$\Delta H_{\text{ads}}^{\circ}$ (kJ mol ⁻¹)	$\Delta S_{\text{ads}}^{\circ}$ (J mol ⁻¹)
303	1.89	-4.98	69.2	244.7
313	3.03	-7.42		
323	3.58	-9.87		

(ΔG°), enthalpy (ΔH°), and entropy (ΔS°) were calculated using the following equations [39]:

$$k_d = \frac{q_e}{C_e} \quad (12)$$

$$\Delta G^{\circ} = \Delta H^{\circ} - T\Delta S^{\circ} \quad (13)$$

$$\ln k_d = \frac{\Delta S^{\circ}}{R} - \frac{\Delta H^{\circ}}{RT} \quad (14)$$

where q_e is the dyes concentration adsorbed on the cross-linked Chi-EGDEB at equilibrium (mg/L), C_e is the equilibrium dyes concentration in the liquid phase (mg/L), and k_d is the distribution coefficient. R is the universal gas constant (8.314 J/mol K) and T is the absolute temperature (K). The values of ΔH° and ΔS° were calculated from the slope and intercept of van't Hoff plots of $\ln k_d$ vs. $1/T$, respectively. The thermodynamic parameters are listed in Table 5. The negative values of ΔG° indicate the adsorption of MO on the cross-linked Chi-EGDEB was spontaneous and more favorable at high temperature [40]. The positive value of the enthalpy change (ΔH°) indicates that the adsorption process is endothermic in nature. The positive entropy change (ΔS°) value corresponds to the increase in the randomness at the solid–solution interface.

4. Conclusion

A cross-linked Chi-EGDEB was developed in the present work for adsorption of MO dye from aqueous solutions. Optimum adsorption conditions of MO were found at adsorbent dosage of 0.3 g/100 mL, and pH 3, and with maximum adsorption capacity of 112.4 mg/g. The Langmuir and Freundlich models were found to fit well with the experimental data. The kinetic data of the MO adsorption under all studied initial concentrations fitted well with the pseudo-second-order kinetic model. Thermodynamic functions show a spontaneous and endothermic nature of the adsorption process. The mechanism of adsorption included mainly hydrogen bonding interaction, electrostatic attractions, and π - π stacking interaction. Thus, cross-linked Chi-EGDEB can be considered a potential for removal of acid dyes from aqueous solution.

References

- [1] G. Sharma, M. Naushad, A. Kumar, S. Rana, S. Sharma, A. Bhatnagar, F.J. Stadler, A.A. Ghfar, M.R. Khan, Efficient

- removal of coomassie brilliant blue R-250 dye using starch/poly (alginate acid-cl-acrylamide) nanohydrogel, *Process Saf. Environ.*, 109 (2017) 301–310.
- [2] A. Kumar, M. Naushad, A. Rana, G. Sharma, A.A. Ghfar, F.J. Stadler, M.R. Khan, ZnSe-WO₃ nano-hetero-assembly stacked on Gum ghatti for photo-degradative removal of Bisphenol A: symbiose of adsorption and photocatalysis, *Int. J. Biol. Macromol.*, 104 (2017) 1172–1184.
- [3] R.A., Rashid, A.H. Jawad, M.A.M. Ishak, N.N. Kasim, KOH-activated carbon developed from biomass waste: adsorption equilibrium, kinetic and thermodynamic studies for Methylene blue uptake, *Desal. Wat. Treat.*, 57 (2016) 27226–27236.
- [4] G. Sharma, A. Kumar, K. Devi, S. Sharma, M. Naushad, A.A. Ghfar, T. Ahamad, F.J. Stadler, Guar gum-crosslinked-Soya lecithin nanohydrogel sheets as effective adsorbent for the removal of thiophanate methyl fungicide, *Int. J. Biol. Macromol.*, 114 (2018) 295–305.
- [5] G. Sharma, A. Kumar, M. Naushad, A. García-Peñas, H. Ala'a, A.A. Ghfar, V. Sharma, T. Ahamad, F.J. Stadler, Fabrication and characterization of Gum arabic-cl-poly (acrylamide) nanohydrogel for effective adsorption of crystal violet dye, *Carbohydr. Polym.*, 202 (2018) 444–453.
- [6] A.H. Jawad, M.A. Islam, B.H. Hameed, Cross-linked chitosan thin film coated onto glass plate as an effective adsorbent for adsorption of reactive orange 16, *Int. J. Biol. Macromol.*, 95 (2017) 743–749.
- [7] M.N. Nawawi, A.H. Jawad, S. Sabar, W.S.W. Ngah, Photocatalytic-oxidation of solid state chitosan by immobilized bilayer assembly of TiO₂-chitosan under a compact household fluorescent lamp irradiation, *Carbohydr. Polym.*, 83 (2011) 1146–1152.
- [8] N.S.A. Mubarak, A.H. Jawad, W.I. Nawawi, Equilibrium, kinetic and thermodynamic studies of Reactive Red 120 dye adsorption by chitosan beads from aqueous solution, *Energy, Ecol. Environ.*, 2 (2017) 85–93.
- [9] A.H. Jawad, M.A. Nawawi, Characterizations of the photocatalytically-oxidized cross-linked chitosan-glutaraldehyde and its application as a sub-layer in the TiO₂/CS-GLA bilayer photocatalyst system, *J. Polym. Environ.*, 20 (2012) 817–829.
- [10] A.H. Jawad, M.A. Nawawi, M.H. Mohamed, L.D. Wilson, Oxidation of chitosan in solution by photocatalysis and product characterization, *J. Polym. Environ.*, 25 (2017) 828–835.
- [11] Y. Wan, K.A. Creber, B. Peppley, V.T. Bui, Ionic conductivity and related properties of crosslinked chitosan membranes, *J. Appl. Polym. Sci.*, 89 (2003) 306–317.
- [12] M. Monier, D.M. Ayad, Y. Wei, A.A. Sarhan, Adsorption of Cu (II), Co (II), and Ni (II) ions by modified magnetic chitosan chelating resin, *J. Hazard. Mater.*, 177 (2010) 962–970.
- [13] W.S. W. Ngah, C.S. Endud, R. Mayanar, Removal of copper (II) ions from aqueous solution onto chitosan and cross-linked chitosan beads, *React. Funct. Polym.*, 50 (2002) 181–190.
- [14] M.L.G. Vieira, M.S. Martinez, G.B. Santos, G.L. Dotto, L.A.A. Pinto, Azo dyes adsorption in fixed bed column packed with different deacetylation degrees chitosan coated glass beads, *J. Environ. Chem. Eng.*, 6 (2018) 3233–3241.
- [15] J. Li, B. Jiang, Y. Liu, C. Qiu, J. Hu, G. Qian, W. Guo, H.H. Ngo, Preparation and adsorption properties of magnetic chitosan composite adsorbent for Cu²⁺ removal, *J. Clean. Prod.*, 158 (2017) 51–58.
- [16] W. Wasim, S. Sagar, A. Sabir, M. Shafiq, T. Jamil, Decoration of open pore network in Polyvinylidene fluoride/MWCNTs with chitosan for the removal of reactive orange 16 dye, *Carbohydr. Polym.*, 174 (2017) 474–483.
- [17] M.A. Nawawi, S. Sabar, A.H. Jawad, Sheilatina, W.S.W. Ngah, Adsorption of Reactive Red 4 by immobilized chitosan on glass plates: towards the design of immobilized TiO₂-chitosan synergistic photocatalyst-adsorption bilayer system, *Biochem. Eng. J.*, 49 (2010) 317–325.
- [18] S. Lagergren, Zur theorie der sogenannten adsorption geloster stoffe, *K. Sven. Vetenskapskad., Handl.*, 24 (1898) 1–39.
- [19] Y.S. Ho, G. McKay, Sorption of dye from aqueous solution by peat, *Chem. Eng. J.*, 70 (1998) 115–124.
- [20] K.Y. Foo, B.H. Hameed, Insights into the modeling of adsorption isotherm systems, *Chem. Eng. J.*, 156 (2010) 2–10.

- [21] M.A. Islam, A. Benhouria, M. Asif, B.H. Hameed, Methylene blue adsorption on factory-rejected tea activated carbon prepared by conjunction of hydrothermal carbonization and sodium hydroxide activation processes, *J. Taiwan Inst. Chem. Eng.*, 52 (2015) 57–64.
- [22] I. Langmuir, The adsorption of gases on plane surfaces of glass, mica and platinum, *J. Am. Chem. Soc.*, 40 (1918) 1361–1403.
- [23] H.M.F. Freundlich, Over the adsorption in solution, *J. Phys. Chem.*, 57 (1906) 385–471.
- [24] M.I. Temkin, V. Pyzhev, Kinetics of ammonia synthesis on promoted iron catalyst, *Acta Phys. Chim. USSR*, 12 (1940) 217–222.
- [25] C. Aharoni, M. Ungarish, Kinetics of activated chemisorption. Part 2.—Theoretical models, *J. Chem. Soc., Faraday Trans. 1 Phys. Chem. Condens. Phases*, 73 (1977) 456–464.
- [26] L. Obeid, A. Bée, D. Talbot, S.B. Jaafar, V. Dupuis, S. Abramson, V. Cabuil, M. Welschbillig, Chitosan/maghemite composite: a magisorbent for the adsorption of methyl orange, *J. Colloid Interface Sci.*, 410 (2013) 52–58.
- [27] A.T. Mohammad, A.S. Abdulhameed, A.H. Jawad, Box-Behnken design to optimize the synthesis of new crosslinked chitosan-glyoxal/TiO₂ nanocomposite: methyl orange adsorption and mechanism studies, *Int. J. Biol. Macromol.*, 129 (2019) 98–109.
- [28] A.A. Jalil, S. Triwahyono, S.H. Adam, N.D. Rahim, M.A.A. Aziz, N.H.H. Hairom, N.A.M. Razali, M.A.Z. Abidina, M.K.A. Mohamadiah, Adsorption of methyl orange from aqueous solution onto calcined Lapindo volcanic mud, *J. Hazard. Mater.*, 181 (2010) 755–762.
- [29] L. Zhai, Z. Bai, Y. Zhu, B. Wang, W. Luo, Fabrication of chitosan microspheres for efficient adsorption of methyl orange, *Chin. J. Chem. Eng.*, 26 (2018) 657–666.
- [30] A.H. Jawad, N.F.H. Mamat, B.H. Hameed, K. Ismail, Biofilm of cross-linked chitosan-ethylene glycol diglycidyl ether for removal of reactive red 120 and methyl orange: adsorption and mechanism studies, *J. Environ. Chem. Eng.*, 7 (2019) 102965.
- [31] R. Huang, Q. Liu, J. Huo, B. Yang, Adsorption of methyl orange onto protonated cross-linked chitosan, *Arab. J. Chem.*, 10 (2017) 24–32.
- [32] H.Y. Zhu, R. Jiang, L. Xiao, G.M. Zeng, Preparation, characterization, adsorption kinetics and thermodynamics of novel magnetic chitosan enwrapping nanosized γ -Fe₂O₃ and multi-walled carbon nanotubes with enhanced adsorption properties for methyl orange, *Bioresour. Technol.*, 101 (2010) 5063–5069.
- [33] R. Jiang, H. Zhu, Y. Fu, Equilibrium and Kinetic Studies on Adsorption of Methyl Orange from Aqueous Solution on Chitosan/Kaolin/ γ -Fe₂O₃ Nanocomposite, In Remote Sensing, Environment and Transportation Engineering (RSETE), International Conference on Remote Sensing, 2011, pp. 7565–7568.
- [34] T.K. Saha, N.C. Bhoumik, S. Karmaker, M.G. Ahmed, H. Ichikawa, Y. Fukumori, Adsorption of methyl orange onto chitosan from aqueous solution, *J. Water Resour. Prot.*, 2 (2010) 898–906.
- [35] J. Zhang, Q. Zhou, L. Ou, Kinetic, isotherm, and thermodynamic studies of the adsorption of methyl orange from aqueous solution by chitosan/alumina composite, *J. Chem. Eng. Data*, 57 (2011) 412–419.
- [36] R. Jiang, Y.Q. Fu, H.Y. Zhu, J. Yao, L. Xiao, Removal of methyl orange from aqueous solutions by magnetic maghemite/chitosan nanocomposite films: adsorption kinetics and equilibrium, *J. Appl. Polym. Sci.*, 125 (2012) 540–549.
- [37] B. Heibati, S. Rodriguez-Couto, A. Amrane, M. Rafatullah, A. Hawari, M.A. Al-Ghouti, Uptake of Reactive Black 5 by pumice and walnut activated carbon: chemistry and adsorption mechanisms, *J. Ind. Eng. Chem.*, 20 (2014) 2939–2947.
- [38] S.K. Singh, A. Das, 2015. The $n \rightarrow \pi^*$ interaction: a rapidly emerging non-covalent interaction, *Phys. Chem. Chem. Phys.*, 17 (2015) 9596–9612.
- [39] G. Karaçetin, S. Sivrikaya, M. Imamoğlu, Adsorption of methylene blue from aqueous solutions by activated carbon prepared from hazelnut husk using zinc chloride, *J. Anal. Appl. Pyrolysis*, 110 (2014) 270–276.
- [40] K.E. Noll, Adsorption Technology for Air and Water Pollution Control, CRC Press, 1991.